

IEEE TRANSACTIONS ON CYBERNETICS

A PUBLICATION OF THE IEEE SYSTEMS, MAN, AND CYBERNETICS SOCIETY

IEEE
SMC

Systems, Man, and Cybernetics Society

Indexed in PubMed® and MEDLINE®, products of the United States National Library of Medicine

PubMed

MEDLINE
U.S. National Library of Medicine

JULY 2020

VOLUME 50

NUMBER 7

ITCEB8

(ISSN 2168-2267)

REGULAR PAPERS

Predicting COVID-19 in China Using Hybrid AI Model	<i>N. Zheng, S. Du, J. Wang, H. Zhang, W. Cui, Z. Kang, T. Yang, B. Lou, Y. Chi, H. Long, M. Ma, Q. Yuan, S. Zhang, D. Zhang, F. Ye, and J. Xin</i>	2891
Command Filter-Based Adaptive NN Control for MIMO Nonlinear Systems With Full-State Constraints and Actuator Hysteresis	<i>J. Qiu, K. Sun, I. J. Rudas, and H. Gao</i>	2905
Event-Triggered Consensus of Linear Multiagent Systems With Time-Varying Communication Delays	<i>C. Deng, M. J. Er, G.-H. Yang, and N. Wang</i>	2916
Fully Distributed Synchronization of Dynamic Networked Systems With Adaptive Nonlinear Couplings	<i>B. Wei, F. Xiao, and Y. Shi</i>	2926
Memristor-Based Neural Network Circuit of Full-Function Pavlov Associative Memory With Time Delay and Variable Learning Rate	<i>J. Sun, G. Han, Z. Zeng, and Y. Wang</i>	2935
Adaptive Neural Event-Triggered Control for Discrete-Time Strict-Feedback Nonlinear Systems	<i>M. Wang, Z. Wang, Y. Chen, and W. Sheng</i>	2946
Lagrange Stability and Finite-Time Stabilization of Fuzzy Memristive Neural Networks With Hybrid Time-Varying Delays	<i>Y. Sheng, F. L. Lewis, Z. Zeng, and T. Huang</i>	2959
Adaptive Neural Control of a Class of Stochastic Nonlinear Uncertain Systems With Guaranteed Transient Performance	<i>J. Wang, Z. Liu, Y. Zhang, C. L. P. Chen, and G. Lai</i>	2971
Tracking Performance Limitations of MIMO Networked Control Systems With Multiple Communication Constraints	<i>C.-Y. Chen, W. Gui, L. Wu, Z. Liu, and H. Yan</i>	2982
Adaptive Consensus Control of Linear Multiagent Systems With Dynamic Event-Triggered Strategies	<i>W. He, B. Xu, Q.-L. Han, and F. Qian</i>	2996
Echo State Network-Based Backstepping Adaptive Iterative Learning Control for Strict-Feedback Systems: An Error-Tracking Approach	<i>Q. Chen, H. Shi, and M. Sun</i>	3009

(Contents Continued on Page 2889)

Distributed Dynamic Event-Triggered Control for Cooperative Output Regulation of Linear Multiagent Systems	Y.-Y. Qian, L. Liu, and G. Feng	3023
Making Sense of Spatio-Temporal Preserving Representations for EEG-Based Human Intention Recognition	D. Zhang, L. Yao, K. Chen, S. Wang, X. Chang, and Y. Liu	3033
Delayed Impulsive Control for Consensus of Multiagent Systems With Switching Communication Graphs	Z.-W. Liu, G. Wen, X. Yu, Z.-H. Guan, and T. Huang	3045
Digital Controller Design via LMIs for Direct-Driven Surface Mounted PMSG-Based Wind Energy Conversion System	P. Mani, J.-H. Lee, K.-W. Kang, and Y. H. Joo	3056
Visual Object Tracking by Hierarchical Attention Siamese Network	J. Shen, X. Tang, X. Dong, and L. Shao	3068
Data-Driven Cyber Security in Perspective—Intelligent Traffic Analysis	R. Coulter, Q.-L. Han, L. Pan, J. Zhang, and Y. Xiang	3081
Distributed Secure Control Against Denial-of-Service Attacks in Cyber-Physical Systems Based on K -Connected Communication Topology	T.-Y. Zhang and D. Ye	3094
Observer-Based Adaptive Fuzzy Decentralized Event-Triggered Control of Interconnected Nonlinear System	Y.-X. Li, S. Tong, and G.-H. Yang	3104
Active Full-Vehicle Suspension Control via Cloud-Aided Adaptive Backstepping Approach	X. Zheng, H. Zhang, H. Yan, F. Yang, Z. Wang, and L. Vlacic	3113
An Improved Fuzzy Sampled-Data Control to Stabilization of T-S Fuzzy Systems With State Delays	X. Wang, J. H. Park, H. Yang, G. Zhao, and S. Zhong	3125
Quasi-Consensus of Heterogeneous-Switched Nonlinear Multiagent Systems	W. Zhang, D. W. C. Ho, Y. Tang, and Y. Liu	3136
Optimal Output Regulation of Linear Discrete-Time Systems With Unknown Dynamics Using Reinforcement Learning	Y. Jiang, B. Kiumarsi, J. Fan, T. Chai, J. Li, and F. L. Lewis	3147
Exponential Stability of Fractional-Order Impulsive Control Systems With Applications in Synchronization	S. Yang, C. Hu, J. Yu, and H. Jiang	3157
Distributed Event-Triggered Consensus of Multiagent Systems With Communication Delays: A Hybrid System Approach	G. Zhao, C. Hua, and X. Guan	3169
ADP-Based Online Tracking Control of Partially Uncertain Time-Delayed Nonlinear System and Application to Wheeled Mobile Robots	S. Li, L. Ding, H. Gao, Y.-J. Liu, L. Huang, and Z. Deng	3182
A Finite-Time Convergent and Noise-Rejection Recurrent Neural Network and Its Discretization for Dynamic Nonlinear Equations Solving	W. Li, L. Xiao, and B. Liao	3195
Distributed Algorithm Design for Nonsmooth Resource Allocation Problems	Z. Deng, X. Nian, and C. Hu	3208
Neural-Network Vector Controller for Permanent-Magnet Synchronous Motor Drives: Simulated and Hardware-Validated Results	S. Li, H. Won, X. Fu, M. Fairbank, D. C. Wunsch, and E. Alonso	3218
Event-Triggered Reinforcement Learning-Based Adaptive Tracking Control for Completely Unknown Continuous-Time Nonlinear Systems	X. Guo, W. Yan, and R. Cui	3231
Robust Adaptive Control Scheme for Teleoperation Systems With Delay and Uncertainties	P. M. Kebria, A. Khosravi, S. Nahavandi, P. Shi, and R. Alizadehsani	3243
Consensus-Based Odor Source Localization by Multiagent Systems Under Resource Constraints	A. Sinha, R. Kumar, R. Kaur, and R. K. Mishra	3254
Necessary and Sufficient Conditions for Consensus of Continuous-Time Multiagent Systems With Markovian Switching Topologies and Communication Noises	M. Li and F. Deng	3264
Event-Triggered Synchronization Strategy for Multiple Neural Networks With Time Delay	J. Chen, B. Chen, Z. Zeng, and P. Jiang	3271
Multisource Transfer Learning for Cross-Subject EEG Emotion Recognition	J. Li, S. Qiu, Y.-Y. Shen, C.-L. Liu, and H. He	3281
Efficient Robust Model Fitting for Multistructure Data Using Global Greedy Search	T. Lai, R. Chen, C. Yang, Q. Li, H. Fujita, A. Sadri, and H. Wang	3294
Lexicographic Multiobjective Scatter Search for the Optimization of Sequence-Dependent Selective Disassembly Subject to Multiresource Constraints	X. Guo, M. Zhou, S. Liu, and L. Qi	3307
Generative Adversarial Networks and Conditional Random Fields for Hyperspectral Image Classification	Z. Zhong, J. Li, D. A. Clausi, and A. Wong	3318
Enhancing Sketch-Based Image Retrieval by CNN Semantic Re-ranking	L. Wang, X. Qian, Y. Zhang, J. Shen, and X. Cao	3330
Local Binary Pattern-Based Adaptive Differential Evolution for Multimodal Optimization Problems	H. Zhao, Z.-H. Zhan, Y. Lin, X. Chen, X.-N. Luo, J. Zhang, S. Kwong, and J. Zhang	3343

Angle-Closure Detection in Anterior Segment OCT Based on Multilevel Deep Network	
..... <i>H. Fu, Y. Xu, S. Lin, D. W. K. Wong, M. Baskaran, M. Mahesh, T. Aung, and J. Liu</i>	3358
Hyperplane Assisted Evolutionary Algorithm for Many-Objective Optimization Problems	
..... <i>H. Chen, Y. Tian, W. Pedrycz, G. Wu, R. Wang, and L. Wang</i>	3367
Weakly Supervised Deep Learning for Brain Disease Prognosis Using MRI and Incomplete Clinical Scores	
..... <i>M. Liu, J. Zhang, C. Lian, and D. Shen</i>	3381
A Distributed Swarm Optimizer With Adaptive Communication for Large-Scale Optimization	
..... <i>Q. Yang, W.-N. Chen, T. Gu, H. Zhang, H. Yuan, S. Kwong, and J. Zhang</i>	3393
Boosting Occluded Image Classification via Subspace Decomposition-Based Estimation of Deep Features	
..... <i>F. Cen and G. Wang</i>	3409

Predicting COVID-19 in China Using Hybrid AI Model

Nanning Zheng, *Fellow, IEEE*, Shaoyi Du[✉], *Member, IEEE*, Jianji Wang[✉], *Member, IEEE*, He Zhang, Wenting Cui[✉], Zijian Kang, Tao Yang, Bin Lou, Yuting Chi, Hong Long, Mei Ma, Qi Yuan, Shupeí Zhang, Dong Zhang, Feng Ye, and Jingmin Xin, *Senior Member, IEEE*

Abstract—The coronavirus disease 2019 (COVID-19) breaking out in late December 2019 is gradually being controlled in China, but it is still spreading rapidly in many other countries and regions worldwide. It is urgent to conduct prediction research on the development and spread of the epidemic. In this article, a hybrid artificial-intelligence (AI) model is proposed for COVID-19 prediction. First, as traditional epidemic models treat all individuals with coronavirus as having the same infection rate, an improved susceptible–infected (SI) model is proposed to estimate the variety of the infection rates for analyzing the transmission laws and development trend. Second, considering the effects of prevention and control measures and the increase of the public’s prevention awareness, the natural language processing (NLP) module and the long short-term memory (LSTM) network are embedded into the SI model to build the hybrid AI model for COVID-19 prediction. The experimental results on the epidemic data of several typical provinces and cities in China show that individuals with coronavirus have a higher infection rate within the third to eighth days after they were infected, which is more in line with the actual transmission laws of the epidemic. Moreover, compared with the traditional epidemic models, the proposed hybrid AI model can significantly reduce the errors of the prediction results and obtain the mean absolute percentage errors (MAPEs) with 0.52%, 0.38%, 0.05%, and 0.86% for the next six days in Wuhan, Beijing, Shanghai, and countrywide, respectively.

Index Terms—Coronavirus disease 2019 (COVID-19) prediction, epidemic model, hybrid artificial-intelligence (AI) model, natural language processing (NLP).

Manuscript received March 14, 2020; revised March 20, 2020; accepted March 26, 2020. Date of publication May 8, 2020; date of current version June 16, 2020. This work was supported by the National Key Research and Development Program of China under Grant 2016YFB1000900. This article was recommended by Associate Editor J. Han. (*Corresponding authors: Nanning Zheng; Shaoyi Du.*)

Nanning Zheng, Shaoyi Du, Jianji Wang, He Zhang, Wenting Cui, Zijian Kang, Tao Yang, Mei Ma, Qi Yuan, Dong Zhang, and Jingmin Xin are with the Institute of Artificial Intelligence and Robotics, Xi’an Jiaotong University, Xi’an 710049, China (e-mail: nnzheng@mail.xjtu.edu.cn; dushaoyi@gmail.com).

Bin Lou, Yuting Chi, Hong Long, and Shupeí Zhang are with the Institute of Artificial Intelligence and Robotics, Xi’an Jiaotong University, Xi’an 710049, China, and also with the School of Software, Xi’an Jiaotong University, Xi’an 710049, China.

Feng Ye is with the Infectious Department, First Affiliated Hospital of Xi’an Jiaotong University, Xi’an 710061, China.

Color versions of one or more of the figures in this article are available online at <http://ieeexplore.ieee.org>.

Digital Object Identifier 10.1109/TCYB.2020.2990162

I. INTRODUCTION

THE OUTBREAK of the coronavirus disease 2019 (COVID-19), which quickly spread across the country, coincided with the spring festival period in China. In its primary stage of transmission, the COVID-19 was not effectively suppressed because of the extreme irregularity of the primary stage of the epidemic, the limited understanding of the new coronavirus by the medical community, and the lack of medical resources [1]. The COVID-19 can be transmitted from person to person, as officially confirmed on January 20, 2020 [2]. Therefore, all provinces and cities in China have implemented strong prevention and control measures, including the closure of the airport and railway stations in Wuhan on January 23, 2020, which are considered the strictest epidemic control measures in history. Public awareness of epidemic prevention has gradually increased because of these effective prevention and control measures. Presently, the number of new infections has decreased significantly. From February 3, 2020 to February 19, 2020, the number of new daily confirmed cases outside Hubei has dropped for 16 consecutive days; the number of new infections in Hubei has also been gradually decreasing since February 12, 2020, and the number of cured patients has increased. The epidemic prevention and control have achieved initial success in China, but in other countries and regions, especially in Europe, Iran, South Korea, the US, and Japan, the epidemic situation is still severe. Every country or region needs to develop targeted prevention and control strategies to control the epidemic effectively. Therefore, conducting research on the development and spread of epidemics is necessary. In the current case, analyzing the development law and predicting the trend of COVID-19 are crucial for effective prevention and control of this epidemic.

When a large-scale epidemic infectious disease emerges and a major public health emergency is initiated, people utilize epidemic models to analyze and predict the development trend of the disease and use the analysis results to guide the development of the prevention and control measures. The most widely used traditional epidemic models are susceptible–infected (SI), SI recovered (SIR), and susceptible–exposed–infected–recovered (SEIR) models [3]–[5], where “S,” “E,” “I,” and “R” denote the number of susceptible people, the number of people in the incubation period, the number of infectious cases, and the number of people who have recovered, respectively. SI, SIR, and SEIR models represent the relationship between I and S in the form of differential equations. These

models have been successfully applied to the prediction of various diseases, such as Ebola and SARS, because of their strong disease prediction capabilities [6]–[10]. Given the severe situation of COVID-19, the analysis of changes in the number of new daily confirmed cases is particularly important for inferring the trend of an epidemic. Therefore, we need to focus on the impact of the trend of new infections on the spread of an epidemic. Furthermore, the influence of cure and mortality rates on the trend of the epidemic are not considered in this article because both parameters have no direct relationship with the number of new daily confirmed cases.

Traditional epidemic models analyze the infection rate based on the dynamic change in the number of infections and subsequently predict the spread and development trend of the epidemic. However, these models consider that all individuals with coronavirus have the same infection rate. Their prediction results can only provide general trends and, thus, have limitations. The government's prevention and control measures have a significant impact on the containment of the development trend of the epidemic, and transparent reporting of the epidemic, implementation of prevention and control measures, and reinforcement of residents' prevention awareness have accelerated the containment of the virus. Evidently, epidemic data alone are insufficient to achieve accurate prediction. We must build a data-driven epidemic model for public health emergencies. By using news information features, we can overcome the limitation of traditional epidemic models that use only a single factor, further improve the accuracy of model prediction, and verify the effectiveness of the government's prevention and control strategies.

To deal with this problem, the long short-term memory (LSTM) network with the natural language processing (NLP) module is introduced into our epidemic model to update the infection rate and further improve the predictive accuracy of the model. LSTM is a classic recurrent neural network (RNN) proposed by Hochreiter and Schmidhuber [11]. LSTM can effectively alleviate gradient explosion and gradient disappearance during the training procedure by introducing the constant error carousel unit. Compared with traditional RNN [12], LSTM exhibits better performance in capturing the long-term dependencies of sequences and is therefore suitable for the classification, processing, and prediction of long-sequence data [13]–[16]. In recent years, LSTMs have been widely used in various tasks, such as NLP [17]–[20]; image generation [21], [22]; and video analysis [23], [24].

This article focuses on the analysis of the infection rate of individuals with coronavirus, models the ability of viruses to infect susceptible people according to different periods after infection, and proposes an improved susceptible–infected (ISI) model. Based on the proposed ISI model, the hybrid artificial-intelligence (AI) model embedded the NLP module and LSTM network for predicting the COVID-19 in this article, and it introduces the important information of the great efforts led by the central government and local governments as well as the massive support participation from the public into the prediction calculation process. Furthermore, this article analyzes the development of the epidemic based on the proposed

hybrid prediction model and predicts the trend of the epidemic. The experimental results obtained based on the epidemic data of several typical provinces and cities in China show that the proposed hybrid model can provide a basis for estimating the law of virus spread, and achieve more accurate and robust performance compared with the traditional epidemic models. Moreover, the prediction results of our hybrid AI model with the introduction of news information are more in line with the actual epidemic development trend, which demonstrates that the openness, transparency, and efficiency of data releasing are very important for establishing a modern epidemic prevention system.

The remainder of this article is organized as follows. Section II introduces the framework of the proposed AI model. Section III proposes the ISI epidemic model to analyze the laws of epidemic transmission. Section IV gives the NLP-based LSTM model for precise prediction. Section V provides the experimental results based on the epidemic data of several typical provinces and cities in China. The conclusion is provided in Section VI.

II. FRAMEWORK OF THE HYBRID AI MODEL

In existing epidemic models, the infection source of new daily confirmed patients in the future consists of those with coronavirus that are not quarantined. Therefore, most epidemic models regard the number of patients who are infected but not quarantined as the base, and then multiply the estimated infection rate to predict the number of new daily confirmed cases [25]–[27]. However, the infection rate of individuals with coronavirus varies at different time intervals of infection [28]. Traditional epidemic models treat all individuals with coronavirus as having the same infection rate and are therefore unable to reflect the evolution trend of an epidemic. Under prevention and control measures, most new confirmed cases at this moment are infected by the new confirmed cases in recent days. Cured and deceased cases are not considered in the establishment of the epidemic model in this article because these cases have no direct impact on the number of new confirmed cases. Based on this assumption, we propose an ISI epidemic model that uses a retrospective approach and a grouped multiparameter method. The basic principle of the retrospective approach is to use the ratio of the number of new confirmed cases at time t to the cumulative number of new confirmed cases over different time scales before time t to calculate the infection rate and establish an epidemic model. Furthermore, the importance of different time scales to the new confirmed cases at time t is analyzed in accordance with the prediction result of the model. Grouped multiparameter factors, which determine the impact of confirmed cases at different times before time t on the confirmed cases at time t , are used to the ISI model to quantify the infection rate of infected cases at different periods. Then, the improved model is used for analyzing the development law of infectious diseases.

In addition, the LSTM network is used to estimate the infection rate deviation of the epidemic model and is combined with the proposed ISI model to estimate the number of

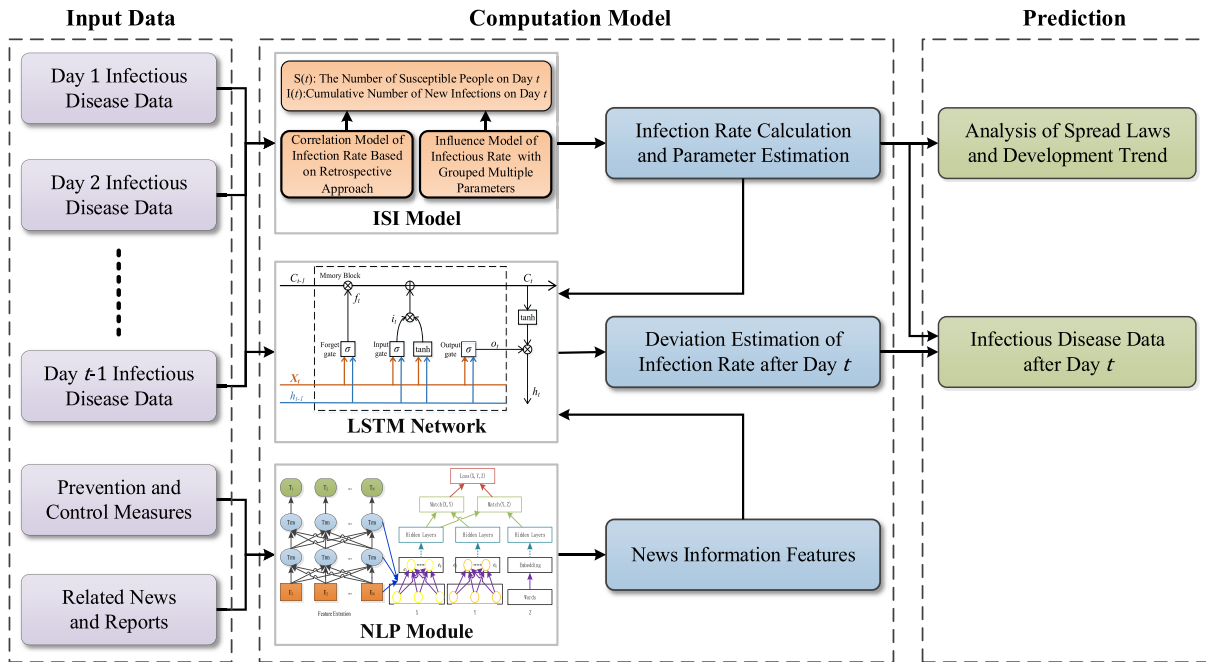


Fig. 1. Hybrid AI model for COVID-19 prediction by using all historical data.

infected cases. To consider the influence of government control measures, the media's transparent reports, and the increase in public awareness regarding epidemic prevention, this article uses pretrained NLP models to extract features from relevant news of various provinces and cities. The extracted features are subsequently combined with the LSTM network to correct the deviation of the infection rate estimated by the ISI model, which could predict the number of infected cases based on the transmission laws and development trend. The proposed framework is shown in Fig. 1.

III. ANALYSIS OF THE LAWS OF EPIDEMIC TRANSMISSION

Traditional epidemic models deem that the number of new infectious cases is related to the number of people who are infected and susceptible, but these models still lack an in-depth analysis. People undergo different infection cycles for different infectious diseases [29]. The time distribution of the infectious sources of new daily confirmed cases must be determined to investigate the infection law of an epidemic. The purpose of this article is to analyze the spread laws and development trend of an epidemic by modeling new confirmed data. However, cure and mortality rates are not directly related to the number of new confirmed cases, so they are not considered in this article.

The observation period for COVID-19 is 14 days [30], so we can posit that almost all new daily confirmed cases are infected by patients confirmed in the past 14 days. Most of the patients under investigation have been quarantined, observed, and tested with a nucleic acid reagent. Patients need to obtain at least two positive results before being confirmed as positive for COVID-19, so we can infer that most of the confirmed patients have been quarantined at least three days prior to the confirmation and are unable to infect others, which means that

most of the confirmed patients cannot be infected by another confirmed case who was confirmed 11 days ago. Therefore, for each day t , this article examines the infection rate of new daily confirmed cases in the past ten days relative to the confirmed cases of day t . For an enhanced analysis, the following symbols are defined: $S(t)$ represents the number of susceptible persons on day t , $I(t)$ represents the cumulative number of confirmed cases of day t (inclusive), and $\Delta I(t) = I(t) - I(t-1)$ represents the number of new confirmed cases on day t .

To obtain a comprehensive understanding of the impact of the infected cases on subsequent infected persons, we need to determine the time interval in which the confirmed cases are most likely to infect the new daily confirmed cases at day t . Then, according to the difference between them, we can determine the laws of transmission. Therefore, in this article, we consider that the patients confirmed on day t are infected by a confirmed person from day $t-1$ to day $t-10$. To determine at which stage the current new daily confirmed cases are infected at a high infection rate, we use the retrospective method to analyze the time laws of epidemic transmission in the past few days. We develop an improved multiparameter epidemic model for the past ten days by applying it to several infection periods and conduct an in-depth analysis of the time laws of the transmission of COVID-19. The framework of the ISI epidemic computational model is shown in Fig. 2.

A. Correlation Model of Infection Rate by Using the Retrospective Method

Traditional epidemic models generally deem that the confirmed cases on a certain day originate from confirmed cases in the past few days. Most of the epidemic models in previous research [31], [32] are based on a fixed number of days and assume that the transmission of an epidemic is affected

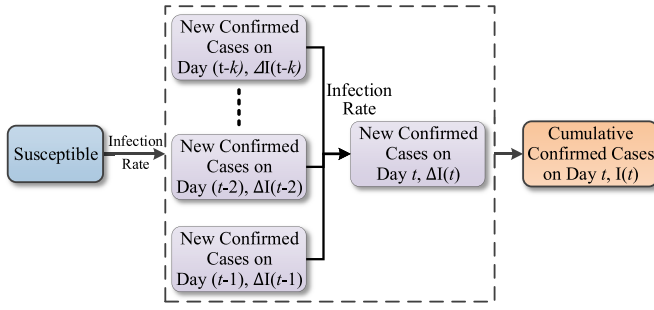


Fig. 2. ISI model.

by previous k days. However, these models lack an in-depth analysis of how epidemics are transmitted. According to the general laws of the development of epidemics, compared with the patients confirmed at the adjacent time (e.g., day $t-1$) on day t , early confirmed patients (e.g., day $t-5$) are more likely to affect patients confirmed on day t . Therefore, by modeling on the infection rate of the cumulative number of confirmed cases in the past k days relative to the confirmed cases on day t , the laws of COVID-19 transmission can be obtained with enhanced macroscopic guiding significance for the overall trend estimation of epidemic development.

We use the retrospective method to analyze the influence of cumulative confirmed cases at different times on the estimation of the infection rate. We examine the infection rate of patients in different regions at different time intervals and investigate whether the current new confirmed cases are infected by the cumulative number of confirmed cases in the past k days. The equation is given as follows:

$$I(t) = I(t-1) + \beta_1(t, k) \sum_{i=1}^k \Delta I(t-i), \quad k = 1, 2, \dots, 10 \quad (1)$$

where $\beta_1(t, k) = \Delta I(t) / \sum_{i=1}^k \Delta I(t-i)$ is the infection rate of the cumulative number of confirmed cases from day $t-k$ to day $t-1$ relative to the new confirmed cases on day t . It reflects the relationship between the number of new confirmed cases $I(t)$ on day t and the number of new confirmed cases $\sum_{i=1}^k \Delta I(t-i)$ in the past k days.

First, the purpose of determining $\beta_1(t, k)$ is to find out the relatively stable relationship between $\Delta I(t)$ and $\sum_{i=1}^k \Delta I(t-i)$, that is, to analyze the impact of the cumulative number of confirmed cases in the past k days on the number of new confirmed cases on day t . The aim is to make the laws of epidemic spread reasonably interpretable and provide support for follow-up work. Second, we can obtain the parameter $\hat{\beta}_1(t, k)$ of each province and the entire country according to (1). Given that the infection rate of epidemics changes exponentially, this article uses the exponential function $L(t) = a \times e^{-bt}$ to fit $\hat{\beta}_1(t, k)$, which can estimate the epidemic spread. In the formula, a and b are the parameters of the exponential function, and $a, b > 0$. Finally, patients have a strong infection rate because they cannot be effectively quarantined during the incubation period. Therefore, this section estimates $\beta_1(t, k)$ by gradually increasing the value of k , and the number of new confirmed cases at an earlier time point is gradually introduced into the model. Then, in accordance with the predictions of the model, we

can analyze whether the new confirmed cases at each time will infect the new confirmed patients on day t . The evolution laws of patients in different time intervals in the process of epidemic transmission can also be obtained.

B. Influence Model of Infection Rate With Grouped Multiparameters

This article considers that infected cases cannot infect the number of susceptible people after being quarantined due to the strict control and quarantine measures. Therefore, the new confirmed cases on day t are most likely to be infected by the new confirmed cases in the past k days. A close relationship exists between the infection rate and the time of infection of patients [33]. Therefore, the new confirmed cases may have different infection rates for the new confirmed cases on day t at different times in the past k days. From (1), we estimate that the most possible infection time dates back to the recent several days. We further analyze this difference and quantify the contribution of new confirmed cases at different times to the infection rate at time t by giving different weights to the number of new confirmed cases each day from day $t-k$ to day $t-1$. Then, we estimate the infection rate by using the weighted cumulative confirmed number, which is adopted to model the epidemic.

To simplify the model, adjacent two days are regarded as a propagation unit, and the same weight α_i is assigned. Multiparameter epidemic modeling is then carried out, as shown in (2). The model avoids the drastic change in weight caused by single data abnormality, thus making the model more robust; at the same time, it reduces the search space of the weight and the complexity of the model

$$I(t) = I(t-1) + \beta_2(t, k) \sum_{i=1}^{k/2} (\alpha_i (\Delta I(t-2i+1) + \Delta I(t-2i))) \quad (2)$$

where $2 \sum_{i=1}^{k/2} \alpha_i = 1$.

Based on the above epidemic model, the model proposed in this section comprehensively considers the difference in the infection rate of new confirmed cases in the past k days relative to the new confirmed cases on day t to study the transmission correlation between the cumulative number of confirmed cases in the past k days and the number of the new cases on day t . First, several groups of different weights α_i are initialized randomly, and a multiparameter epidemic model is established by (2). The better the prediction result of the model, the better the corresponding weights reflect the real infection law. Finally, the infection rate with a great contribution to the virus infection can be inferred by comparing the weights assigned to different time points.

We obtain the relationship between the new confirmed cases on day t and the new confirmed cases on days $t-10$ to $t-1$ through the value of α_i on the basis of (1) and (2). However, too few parameters can cause underfitting [i.e., (1)], while too many parameters can easily cause overfitting [i.e., (2)]. Therefore, we further balance the number of parameters based on the above results. The set of days $\{t-i | i = 1, 2, \dots, 10\}$ is

divided into two groups, where the set of days with a greater impact on the new confirmed cases on day t is recorded as set A , and the remaining days are recorded as set B . Set A is given weight γ_1 , and set B is given weight γ_2 , as in

$$I(t) = I(t-1) + \beta_3(t) \left(\gamma_1 \sum_{t_1 \in A} \Delta I(t_1) + \gamma_2 \sum_{t_2 \in B} \Delta I(t_2) \right) \quad (3)$$

where $\gamma_1|A| + \gamma_2|B| = 1$, $|\cdot|$ denotes the number of elements in a set. We calculate the infection rate according to (3).

C. Data Preprocessing Method Based on the Proposed Model

The diagnostic criteria for patients at the beginning of the outbreak of COVID-19 changed throughout the country due to insufficient medical resources and limited understanding of the clinical signs of the novel coronavirus. These factors led to the presence of considerable noise in the epidemic data of all provinces. Hubei Province incorporated clinical diagnosis into the diagnostic criteria after the fifth edition of the treatment and diagnosis plan was released on February 12, 2020. This clinical diagnosis caused the new daily confirmed cases of Wuhan to surge to 13 436 on that day. These abnormal and noisy data points bring great difficulties to subsequent modeling.

Data cleaning (i.e., removing abnormal data points) and the interpolation-based method are two widely applied approaches to deal with anomalous data points. However, these methods have many drawbacks. Data cleaning causes serious data loss and reduces the accuracy of the overall trend estimation of the epidemic model because the time scale of the epidemic data is extremely small. Meanwhile, although the interpolation-based method does not cause data loss, it loses the dynamic evolution laws of abnormal dates and affects the accuracy of short-term parameter estimation. Therefore, most of the new daily confirmed cases from abnormal data points are missed diagnoses from the early stage of the epidemic. Ignoring this number of patients will force the model to be too optimistic about the epidemic status of the early stage of the outbreak and will affect the modeling of subsequent evolution laws. For the abnormal data points near February 12, 2020, this article proposes a “data balance” method based on the epidemic model as a data preprocessing module to reduce the impact of changes in diagnostic criteria.

First, the data before February 12, 2020 are applied to build an epidemic model to predict the number of new daily confirmed cases on the anomaly dates. Second, the difference between all actual data points and the prediction results is summed up as the number of early missed patients. Third, these patients are evenly divided into abnormal and normal dates to achieve “trend balance” of the overall data. The implementation details are as follows.

- 1) Let the date with abnormal data start at t_s and end at t_e . Use $I(t_0) \cdots I(t_s)$ to establish an ISI epidemic model and predict the number of new daily confirmed cases on abnormal dates $\hat{\Delta I}(t_s) \cdots \hat{\Delta I}(t_e)$.
- 2) Calculate the total number of missed diagnoses M and the cumulative number of new daily confirmed cases of

the early stage N

$$\begin{aligned} M &= \sum_{t=t_s}^{t_e} (\Delta I(t) - \hat{\Delta I}(t_s)) \\ N &= \sum_{t=t_0}^{t_s-1} \Delta I(t) + \sum_{t=t_s}^{t_e} \hat{\Delta I}(t). \end{aligned} \quad (4)$$

- 3) Let $\alpha = M/N$. Then, the rebalanced data before t_e can be obtained by the following equation:

$$\begin{cases} \Delta I'(t) = (1 + \alpha)\Delta I(t), & t = t_0, \dots, t_s - 1 \\ \Delta I'(t) = (1 + \alpha)\hat{\Delta I}(t), & t = t_s, \dots, t_e. \end{cases} \quad (5)$$

The data balance preprocessing method has two main advantages.

- 1) The evolution trend of $\beta(t)$ will not be affected according to the calculation method [i.e., (1)–(3)] of the infection rate $\beta(t)$ if the numbers of the new daily confirmed cases before t_s are increased α times.
- 2) The number of new daily confirmed cases $I(t)$ before and after the anomaly date can maintain its evolution trend after all the data points before t_e have been enlarged; therefore, the long-term fitting result of $\beta(t)$ becomes increasingly stable. We select t_s as February 12, 2020 and t_e as February 13, 2020.

IV. PREDICTION OF THE DEVELOPMENT TREND OF THE EPIDEMIC

The epidemic model can predict the spread of infectious diseases well but does not consider other factors, such as prevention and control measures, which prevent the spread of infectious diseases. Therefore, new mechanisms need to be introduced to update the parameters in the epidemic model. The LSTM network can be used to model hidden variables (e.g., number of potentially infected people) and is often utilized for data prediction. However, experiments have proven that using the LSTM network alone to predict the number of infected cases is not an effective method. Considering that the prevention and control measures and people’s awareness of epidemic prevention are closely related to the spread of the virus, this article uses the NLP technology to extract semantic features from news reports related to prevention and control measures and people’s attitudes toward the epidemic. These features are then used in the LSTM network. The number of infections is predicted by revising the infection rate in the traditional epidemic model. This method maintains the long-term trend of infectious disease models and updates the infection rate through the usage of news information to improve the accuracy of epidemic prediction.

We collect news information related to the epidemic situation in China. From this information, text data related to prevention and control measures are extracted. The extracted titles and profiles are converted into feature vectors by using a pretrained NLP model. We also extract the features in news information through NLP and combine the LSTM network to update the deviation of the infection rate in the ISI model and achieve an accurate prediction of the number of infections, which is shown in Fig. 3.

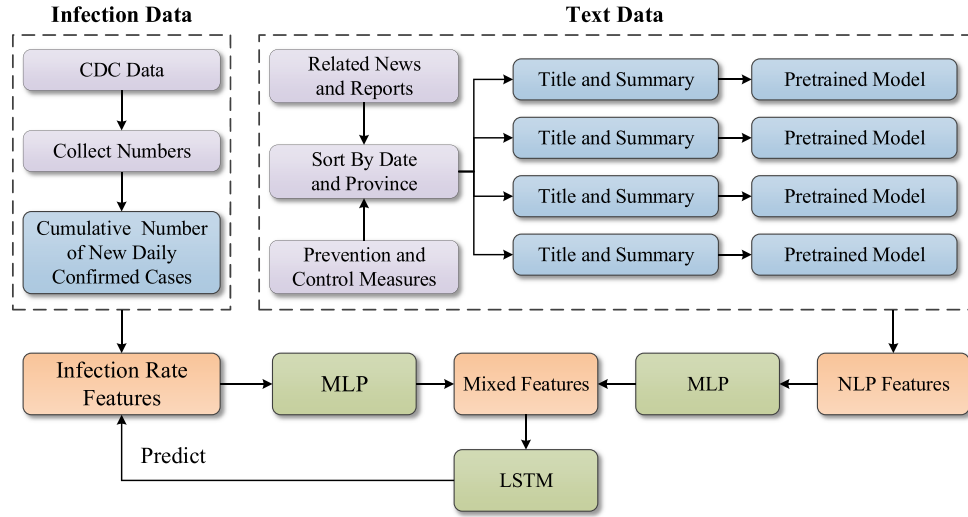


Fig. 3. Prediction model based on the infection rate and NLP features (MLP: multilayer perceptron, NLP: natural language processing, LSTM: long short-term memory network, and CDC: centers for disease control).

A. News Feature Extraction

To extract the relevant features of news information, we examine the information related to the COVID-19, sort this information by date, province, and city, and filter out case reports and related foreign news. Feature extraction is only performed on the title and main content of each news text to obtain concise and robust features in practice. For each given news text in Chinese, a pretrained model of the BERT language model (RoBERTa) [34], which was designed by researchers at Facebook AI and the University of Washington, is used to extract text features. This model combines the Chinese Whole Word Masking strategy, uses WordPiece segmentation to divide a complete word into several subwords, and also combines BERT. This model can achieve good feature extraction results with minimal training.

The news titles and main content are separately obtained as the input to prevent overfitting and achieve efficient training, and the last hidden layer of the pretrained model is used to encode the text. Then, we encode 768-D title and 768-D text together to generate a 1536-D NLP feature vector, in which each vector corresponds to a piece of news. The dataset is divided into national and provincial datasets to achieve accurate daily predictions in different cities and regions and the entire country, where the national dataset contains news from all regions, and the provincial dataset contains news from each province. The news is classified by day to ensure the presence of at least one news per day, and the features of all news of the day are averaged as the NLP feature vector.

B. LSTM Network Based on NLP and Infection Rate

Deep neural networks have the capacity to fit complex distributions but tend to overfit without sufficient supervision. As infection rate features are based on the growing percentage of each factor, they are stable across time. However, epidemic models based on the infection rate cannot predict policy changes and emergency conditions nor adjust the prediction with short-term influence. Therefore, we introduce the LSTM

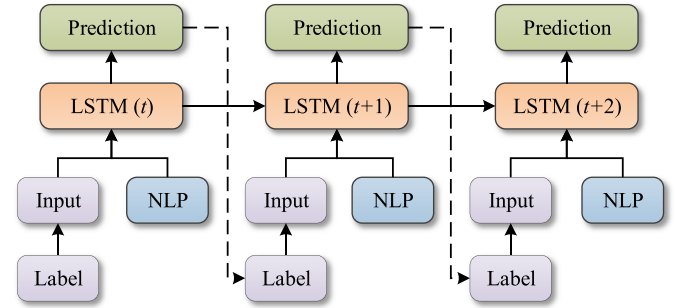


Fig. 4. LSTM network based on NLP features.

network based on NLP features to model the current policy and social media, which is shown in Fig. 4. Then, the short-term flexibility and long-term stability are both ensured.

In the ISI model, we assume that the actual infection rate is $\beta(t)$, and the infection rate that regressed under the exponential function is $\hat{\beta}(t)$. We use the neural network to predict the bias between the actual infection rate and the regressed infection rate. We let the label of day t be $y(t) = \beta(t) - \hat{\beta}(t)$, which is taken as the bias feature for prediction. Therefore, we can use the LSTM network as a complement to the ISI model.

To take the impact of news and policies into consideration, we combine the NLP features introduced in Section IV-A with the bias features. We use LSTM to encode temporal information and hidden states. We adopt a one-layer perception model (with a fully connected layer and a leaky ReLU activation function) to transform the infection and NLP features into 32-D vectors. This approach ensures that two features provide the same contribution to our network.

Given infection features s_1 and NLP features s_2 , let the weight of the first two perception model be W_1 and W_2 . Let $g(\cdot)$ be the function of convolution and leaky ReLU as follows:

$$\begin{aligned} f_1 &= g(s_1; W_1) \\ f_2 &= g(s_2; W_2). \end{aligned} \quad (6)$$

The processed features are f_1 and f_2 , which are concatenated into a mixed feature f . At every timestamp t , assuming that the given hidden state from timestamp $t - 1$ is h_{t-1} , let the mixed feature be $f(t)$. Function lstm includes the LSTM network and the fully connected layer that transforms the hidden state into prediction. The output of the network is $x(t)$ and the new hidden state $h(t)$. Then

$$(x(t), h(t)) = \text{lstm}(f(t), h(t - 1); W_l) \quad (7)$$

where W_l is the weight of the network. We use gradient descent and the Adam optimizer [35] as the optimization method during training. Then, the mean-square error between prediction and label is adopted as the loss function.

V. EXPERIMENTAL RESULTS

In this section, the performance of the proposed model is evaluated on the epidemic data, which are sourced in two ways. First, most of the data mainly come from the national and provincial health commissions and include the numbers of people who are infected, suspected, cured, and have died. Second, data for NLP are obtained from dxy.com [36], social media, and news media. We filter foreign news and disease reports first and then classify the media by the dates and relevant provinces.

A. Correlation Analysis of Cumulative Daily Confirmed Cases and Infection Rate

The infection rate of viruses is deemed to be periodic in existing epidemic models [37]. Considering that patients who have been diagnosed are strictly medically isolated and no longer have the conditions to infect others, we assume that the majority of the sources of infection at day t come from the cumulative new daily confirmed cases in the previous k days. An epidemic model based on a retrospective method is used to analyze the epidemic data of Beijing, Shanghai, and Hunan and further explore the dynamic transmission laws of the virus.

Some patients were missed or misdiagnosed in the early stage of COVID-19 due to the lack of medical resources and changes in diagnostic criteria in certain cities. These factors introduced some noise to the epidemic data. To reduce the impact of noise, we select Shanghai, where public health facilities are relatively complete, as the research object and analyze the evolution laws of the infection rate of the COVID-19. We initially select k time scales to model the correlation between infection rate β_1 and cumulative confirmed cases; then, we analyze the infection rate of the confirmed cases at different time intervals according to the prediction results. The experimental results are of great importance for us to infer the evolutionary trend of the epidemic and estimate the laws of virus infection.

The results of the exponential fitting curves of the estimated infection rate in Shanghai against the different values of k are shown in Fig. 5. Moreover, to quantitatively assess the best value of k determining the infection rate, we use the fitted infection rate to estimate the number of the predicted cumulative confirmed cases. The mean absolute error (MAE)

curves between the number of actual cumulative confirmed cases and the number of predicted cumulative confirmed cases for Shanghai are shown in Fig. 6. The infection rate of each epidemic model is obtained from the results of the exponential fitting, and the time scale of the data used for the infection rate fitting is from January 23, 2020 to February 18, 2020. As shown in Fig. 5 and the curve of Shanghai in Fig. 6, when k is small ($k = 1-3$), the distribution of infection rate β_1 does not show apparent regularity, and the prediction result of the number of cumulative confirmed cases has a relatively large error. This finding shows that the new daily confirmed cases of dates near day t have a weak impact on the infection rate. As k gradually increases ($k = 4-6$), the distribution of infection rate β_1 becomes concentrated, and the estimation error of the epidemic model decreases rapidly. This observation proves that the trend of infection rate β_1 gradually approaches the truth, and the dates with a significant effect on day t are gradually incorporated into the model. When k is greater than 7, the distribution of β_1 no longer changes significantly, but the MAE curve of the epidemic model gradually increases, proving that the trend of β_1 begins to deviate from the truth. This deviation indicates that noisy data have been introduced into the model, that is, the patients at day $t - k$ have been isolated and no longer infect the S group at day t .

We also establish two epidemic models for patients' data in Beijing and Hunan to verify the generality of the above-mentioned laws. The MAE curves of the two regions are also shown in Fig. 6. According to the performance of the epidemic models, the exponential fitting effect of the infection rate in the two regions is similar to an inverted bell curve, which further validates that the impact of the new daily confirmed cases on the infection rate varies at different dates. The new daily confirmed cases in the middle phase during the period from $t - 10$ to $t - 1$ have a great impact on the infection rate of time t .

The experimental results of the aforesaid provinces and cities reflect the general development trend of the epidemic, but the change in the diagnosis criteria on February 12, 2020 led to a sharp increase in the number of new daily confirmed cases in Wuhan. To resolve this problem, we initially establish an epidemic model based on data from January 23, 2020 to February 11, 2020 in Wuhan and use the exponential function to fit the overall evolution trend of the infection rate. As shown in Fig. 7, the fitting curve of Wuhan's infection rate is similar to that of Shanghai and Beijing, that is, the trend of the epidemic in Wuhan is also stable. Therefore, using the data balance method described in Section III-C to preprocess the anomaly data points in Wuhan is reasonable.

B. Analysis of the Influence on the Infection Rate of New Confirmed Cases at Different Time Intervals

Patients in incubation at different infection time intervals have different infection rates [38], [39]. The new daily confirmed cases from day $t - k$ to day $t - 1$ may have different influences on the infection rate of the newly confirmed patients on day t . Here, we investigate the influence and time

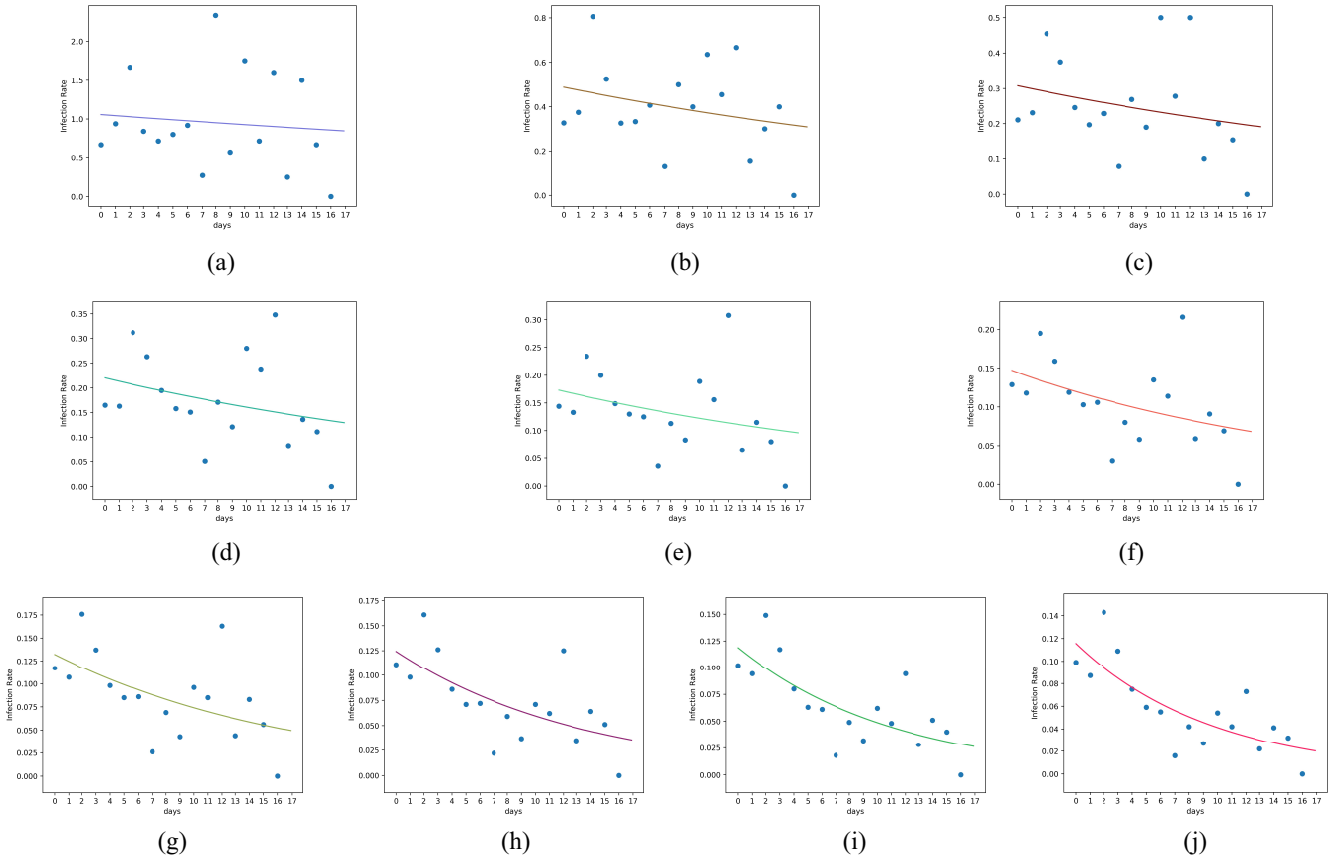


Fig. 5. Fitting curves of infection rate β_1 in Shanghai. (a) $k = 1$. (b) $k = 2$. (c) $k = 3$. (d) $k = 4$. (e) $k = 5$. (f) $k = 6$. (g) $k = 7$. (h) $k = 8$. (i) $k = 9$. (j) $k = 10$.

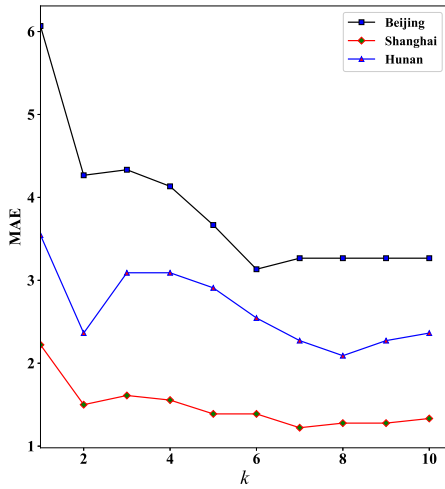


Fig. 6. MAE curves between the number of actual cumulative confirmed cases and the number of predicted cumulative confirmed cases in Shanghai, Beijing, and Hunan.

laws of epidemic transmission in the different provinces and cities by using (2).

We begin by analyzing the relationship between the new confirmed cases in the past ten days and the new daily confirmed cases on day t in Beijing, Shanghai, Zhejiang, and Hunan. Similar to the conclusions in the above section, the curve of parameter α is generally similar to a bell curve when

the distribution of weights is considered. That is, the new confirmed cases from day $t - 8$ to day $t - 3$ have a larger contribution to the new confirmed cases on day t , whereas the contribution rates of the new confirmed cases from $t - 10$ to $t - 9$ and from $t - 2$ to $t - 1$ are smaller, as shown in Fig. 8(a).

When (2) is used to fit the estimated parameter $\beta_2(t)$, the distribution of α_i shows a trend where the value is small on both sides and large in the middle. Meanwhile, the value of α_i on day $t - 10$ is close to 0, indicating that the earlier confirmed cases have little influence on the confirmed cases on day t . Further study reveals that α_i on days $t - 8$ to $t - 3$ is larger, whereas those on days $t - 10$ to $t - 9$ and days $t - 2$ to $t - 1$ are smaller for most provinces and cities. Therefore, the average infection time is about 5.5 days.

To avoid underfitting or overfitting phenomenon analyzed in Section V-A, we balance the parameters via a grouped multi-parameter strategy. According to (3), the weights of the dates from $t - 8$ to $t - 3$ can be set as the same parameter γ_1 , and the weights of the days $t - 10$ to $t - 9$ and $t - 2$ to $t - 1$ can be set as the same parameter γ_2 . Then, (3) can be converted to

$$I(t) = I(t-1) + \beta_2(t)\gamma_1 \sum_{i=3}^8 \Delta I(t-i) + \beta_2(t)\gamma_2 \left(\sum_{i=1}^2 \Delta I(t-i) + \sum_{i=9}^{10} \Delta I(t-i) \right) \quad (8)$$

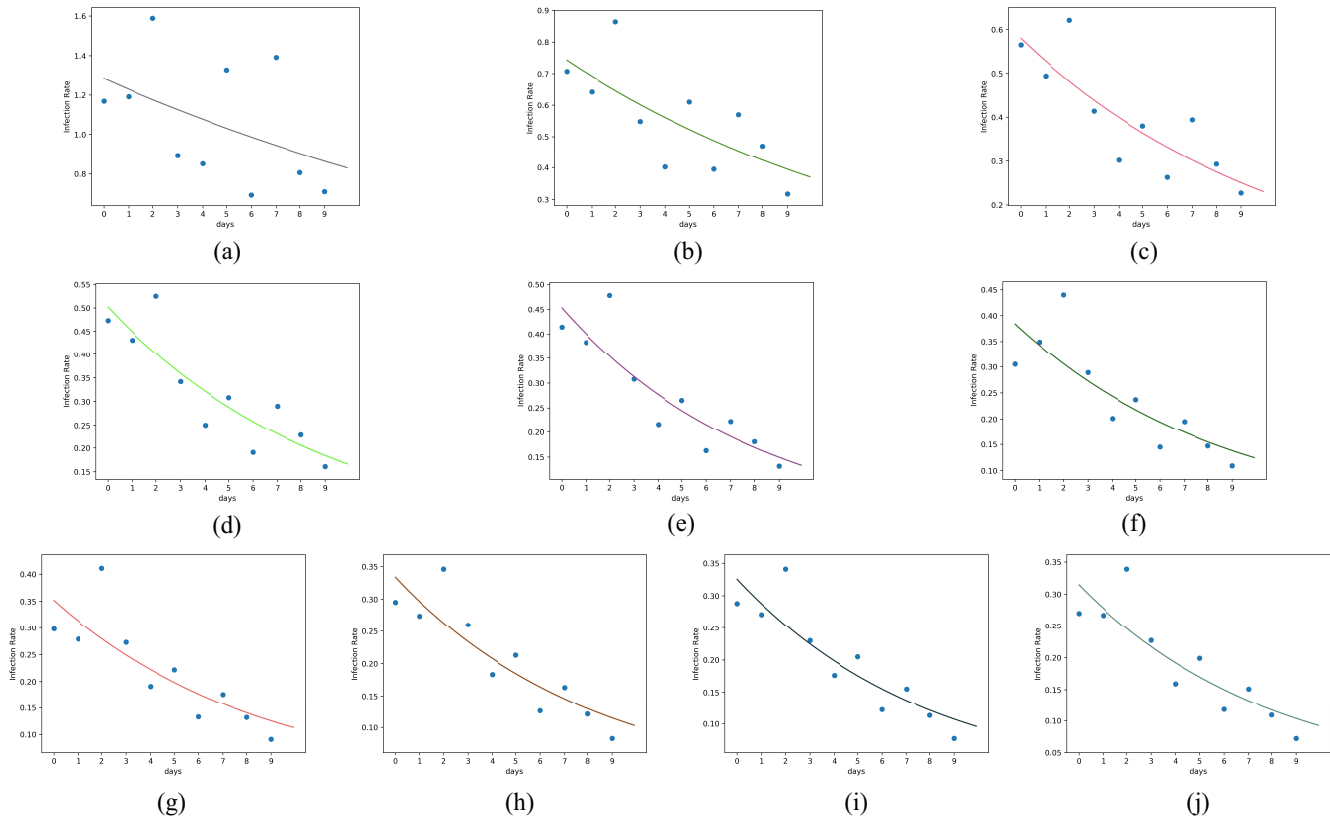


Fig. 7. Fitting curves of infection rate β_1 in Wuhan. (a) $k = 1$. (b) $k = 2$. (c) $k = 3$. (d) $k = 4$. (e) $k = 5$. (f) $k = 6$. (g) $k = 7$. (h) $k = 8$. (i) $k = 9$. (j) $k = 10$.

where $6\gamma_1 + 4\gamma_2 = 1$. According to this equation, we have the results as shown in Fig. 8.

It shows a consistent distribution in the different provinces and cities in Fig. 8. We can see that the values of γ_2 are always less than the values of γ_1 for all the curves in Fig. 8. For Zhejiang and Hunan, γ_2 is close to zero. For other cities, we take the values of γ_2 as a noise and set γ_2 as zero. Finally, we can reformulate (3) as follows:

$$I(t) = I(t-1) + \beta_4(t) \sum_{i=3}^8 \Delta I(t-i). \quad (9)$$

C. Prediction of the Cumulative Number of COVID-19 Cases

We verify our model in Wuhan, Beijing, Shanghai, and countrywide. The numbers of preprocessed infections from January 23, 2020 to February 18, 2020 are used as the training data to predict the number of infections from February 19, 2020 to February 24, 2020.

To verify the effectiveness of our model and the influence of government control and public awareness of epidemic prevention, we compare the traditional IS model, the ISI model, the ISI model with the LSTM network, and the ISI model with NLP features and the LSTM network. The NLP features extracted from the current and past news are used in the LSTM network. We compare the daily prediction, MAE, and mean absolute percentage error (MAPE) for Wuhan, Beijing,

TABLE I
COMPARISON OF ACTUAL CONFIRMED NUMBER AND PREDICTED NUMBER IN WUHAN

	SI	ISI	ISI+LSTM	ISI+NLP+LSTM	GT
Feb. 19	45794	45260	45175	44970	45027
Feb. 20	47030	45997	46307	45504	45346
Feb. 21	48130	46628	46918	45872	45660
Feb. 22	49106	47138	47665	46163	46201
Feb. 23	49970	47532	48045	46265	46607
Feb. 24	50732	47842	48538	46439	47071
MAE	2475.00	747.50	1122.67	239.83	0
MAPE	5.35%	1.62%	2.43%	0.52%	0

TABLE II
COMPARISON OF ACTUAL CONFIRMED NUMBER AND PREDICTED NUMBER IN BEIJING

	SI	ISI	ISI+LSTM	ISI+NLP+LSTM	GT
Feb. 19	396	394	394	395	395
Feb. 20	398	395	395	396	396
Feb. 21	400	396	396	397	399
Feb. 22	402	396	396	397	399
Feb. 23	403	397	397	397	399
Feb. 24	404	397	398	397	400
MAE	2.50	2.17	2.00	0.50	0
MAPE	0.63%	0.54%	0.50%	0.38%	0

Shanghai, and countrywide. We round off the prediction results for simplicity, and the compared results are shown in Tables I–IV.

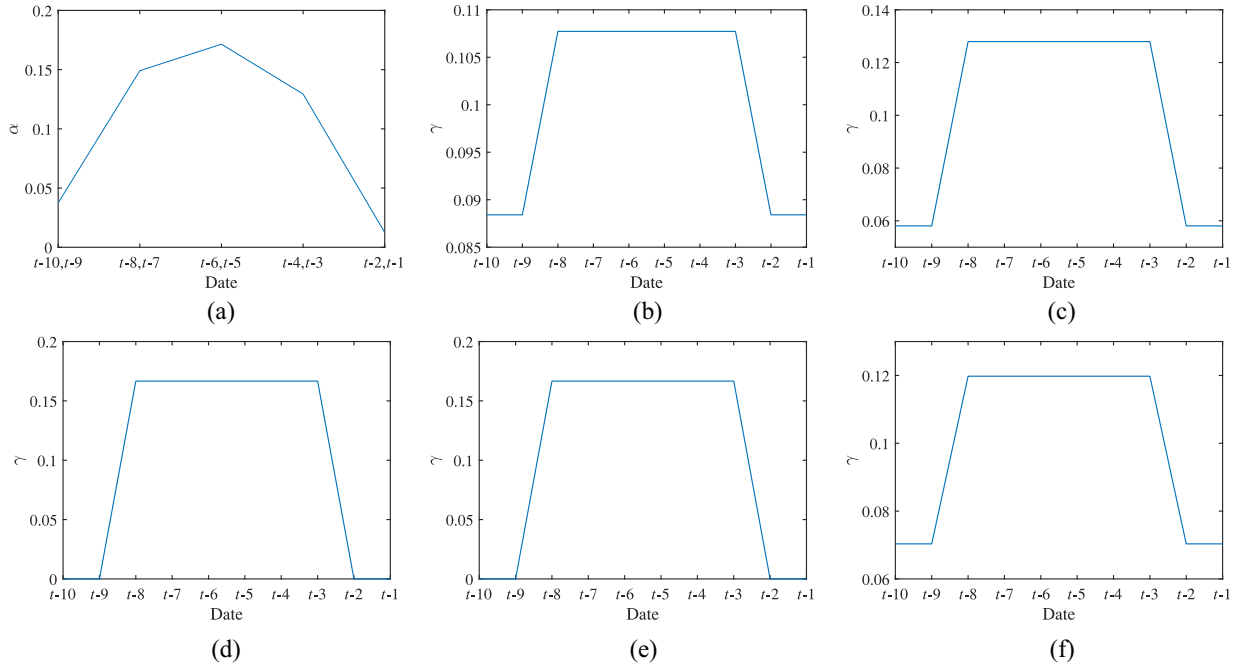


Fig. 8. Infection rate of the new confirmed cases from day $t - 10$ to $t - 1$ to new confirmed cases on day t in the different provinces or cities and the average effect, where “Average” denotes the average contribution of newly confirmed cases from $t - 10$ to $t - 1$ to new confirmed cases on day t in four regions: Beijing, Shanghai, Zhejiang, and Hunan. (a) Average. (b) Beijing. (c) Shanghai. (d) Zhejiang. (e) Hunan. (f) Wuhan.

TABLE III

COMPARISON OF ACTUAL CONFIRMED NUMBER AND PREDICTED NUMBER IN SHANGHAI

	SI	ISI	ISI+LSTM	ISI+NLP+LSTM	GT
Feb. 19	336	334	334	334	333
Feb. 20	338	335	335	334	334
Feb. 21	340	335	335	334	334
Feb. 22	341	336	336	335	335
Feb. 23	343	336	337	335	335
Feb. 24	344	336	337	335	335
MAE	6.00	1.00	1.33	0.17	0
MAPE	1.79%	0.30%	0.40%	0.05%	0

TABLE IV

COMPARISON OF ACTUAL CONFIRMED NUMBER AND PREDICTED NUMBER AT THE COUNTRYWIDE SCALE

	SI	ISI	ISI+LSTM	ISI+NLP+LSTM	GT
Feb. 19	75902	75368	75536	75270	74576
Feb. 20	77431	76396	76668	76116	75465
Feb. 21	78787	77210	77621	76807	76288
Feb. 22	79988	77817	78393	77432	76936
Feb. 23	81049	78290	79009	77970	77150
Feb. 24	81984	78667	79510	78432	77658
MAE	2844.67	945.83	1444.00	659.00	0
MAPE	3.71%	1.24%	1.89%	0.86%	0

Our model makes decent predictions for the three typical cities, as described in Fig. 9. Our ISI model makes a remarkable improvement of the traditional SI model. Compared with the ISI model, the LSTM network is not consistently improved, which is unstable. The ISI+NLP+LSTM achieves a more precise prediction than the other models. This finding shows that NLP features provide extra information and guidance for disease prediction.

In summary, based on the ISI model, the hybrid AI model for predicting the COVID-19 proposed in this article is embedded with the NLP module, which introduced the important information of the great efforts led by the central government and local governments as well as the massive support participation from the public into the prediction calculation process, so that the prediction results are more in line with the actual epidemic development trend.

D. Basic Reproduction Number R_0

Basic reproduction number R_0 is a widely applied epidemiologic metric to describe the transmissibility of an infectious patient. In this article, the basic reproduction number $R_0(t)$ is defined as the average number of secondary cases that one confirmed case at time t would produce in a completely susceptible population. According to (9), it is formulated as follows:

$$I(t+j) = I(t+j-1) + \beta_4(t+j) \sum_{i=3}^8 \Delta I(t+j-i). \quad (10)$$

According to the above equation, the secondary cases infected by the new daily confirmed cases at time t consist of $\beta_4(t+3)\Delta I(t)$, $\beta_4(t+4)\Delta I(t)$, \dots , $\beta_4(t+8)\Delta I(t)$. Thus, the basic reproduction number at time t can be calculated as

$$R_0(t) = \frac{\sum_{i=3}^8 [\beta_4(t+i)\Delta I(t)]}{\Delta I(t)} = \sum_{i=3}^8 \beta_4(t+i). \quad (11)$$

We analyze the evolutionary trends of the basic reproduction number R_0 in Beijing, Shanghai, Zhejiang, Hunan, and Wuhan, as shown in Fig. 10, from which we can see that the values of

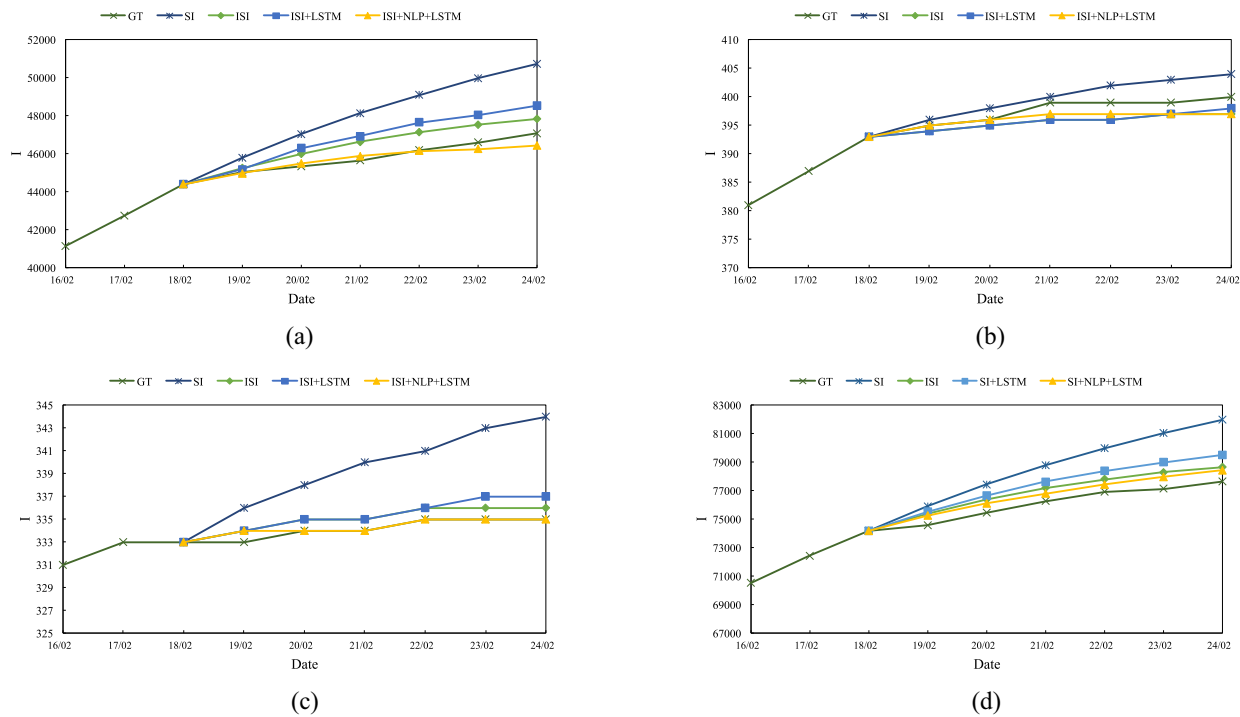


Fig. 9. Comparison of actual confirmed number and predicted number in three typical cities and at the countrywide scale. (a) Wuhan. (b) Beijing. (c) Shanghai. (d) Countrywide.

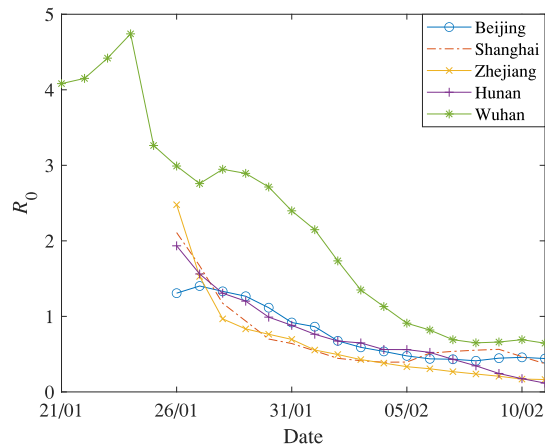


Fig. 10. Curves of the basic reproduction number R_0 for different provinces and cities in China.

R_0 for all regions gradually decrease with the implementation of prevention and control measures.

The Wuhan area was locked down on January 23, 2020, which was a crucial time point of the COVID-19 epidemic. To analyze the impact of the lockdown of the city on R_0 , we analyze more values of R_0 for Wuhan. As shown in Fig. 10, the R_0 curve in Wuhan peaked on January 24, 2020 then dropped rapidly, indicating that locking down the city played an essential role in curbing the spread of the COVID-19. With the proposed hybrid AI model, we also make a prediction about the cumulative confirmed cases in Wuhan, and all of China, the data used for prediction were collected from January 23, 2020 to February 18, 2020. The prediction curves of the cumulative confirmed cases are shown in Fig. 11, from which we can see

that the number of cumulative confirmed cases till the end of March would be 48 247 for Wuhan. However, if Wuhan was locked down on January 27, 2020, with a delay of four days of the actual time, the number would increase to 102 769.

VI. CONCLUSION

This article, which aims to predict the trend of the COVID-19, discovered that new daily confirmed cases at different time intervals have different contributions to susceptible infections. The impact of confirmed cases in the past several days before time t on the new daily confirmed cases at time t is analyzed. On this basis, we propose a grouped multiparameter strategy that sets the infection rates of the confirmed cases in the past into different groups by time. Then, we derive the proposed ISI model with multiple parameters. This article uses NLP technology to analyze and extract related news information, such as epidemic control measures and residents' awareness of epidemic prevention, which are then encoded into semantic features. Then, these features are fed to the LSTM network to update the infection rate given by the ISI model.

In summary, based on the ISI model, the hybrid AI model for predicting the COVID-19 proposed in this article is embedded with the NLP module, which introduced important information led by the great efforts of the central government and local governments as well as the massive support participation from the public into the prediction calculation process. The prediction results of the model are highly consistent with actual epidemic cases, which proves that the proposed hybrid model can more accurately analyze the transmission law and development trend of the virus compared with previous models and that language information processing of related news can

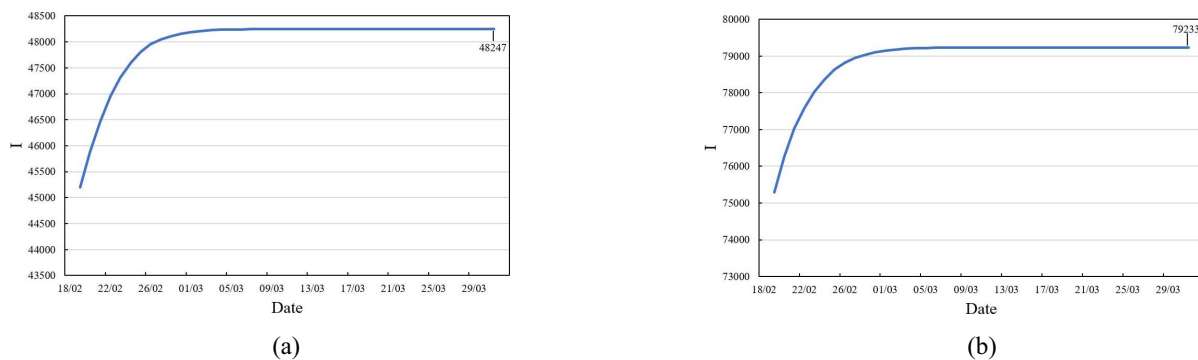


Fig. 11. Prediction curves of the cumulative confirmed cases in (a) Wuhan and at the (b) countrywide scale.

help improve the accuracy of the prediction model. In addition, we provide an effective method for the prediction of the transmission law and development trend of public health events in the future. This article also shows that the openness, transparency, and efficiency of releasing data are very important for establishing a modern epidemic prevention system.

ACKNOWLEDGMENT

The authors would like to thank Dr. P. Hu of the School of Management, Xi'an Jiaotong University, for her discussion and constructive comments for our research framework.

REFERENCES

- [1] S. Ying *et al.*, "Spread and control of COVID-19 in China and their associations with population movement, public health emergency measures, and medical resources," p. 24, Feb. 2020. [Online]. Available: <https://doi.org/10.1101/2020.02.24.20027623>
- [2] Y. Bai *et al.*, "Presumed asymptomatic carrier transmission of COVID-19," *JAMA*, vol. 323, no. 14, pp. 1406–1407, 2020.
- [3] W. O. Kermack and A. G. McKendrick, "A contribution to the mathematical theory of epidemics," *Proc. Royal Soc. London Ser. A, Contain. Papers Math. Phys. Character*, vol. 115, no. 772, pp. 700–721, 1927.
- [4] M. Y. Li, J. R. Graef, L. Wang, and J. Karsai, "Global dynamics of a SEIR model with varying total population size," *Math. Biosci.*, vol. 160, no. 2, pp. 191–213, 1999.
- [5] Z. Yang *et al.*, "Modified SEIR and AI prediction of the epidemics trend of COVID-19 in China under public health interventions," *J. Thorac. Dis.*, vol. 12, no. 23, pp. 165–174, 2020.
- [6] T. Berge, J.-S. Lubuma, G. Moremedi, N. Morris, and R. Kondera-Shava, "A simple mathematical model for Ebola in Africa," *J. Biol. Dyn.*, vol. 11, no. 1, pp. 42–74, 2017.
- [7] C. Rizkalla, F. Blanco-Silva, and S. Gruver, "Modeling the impact of Ebola and bushmeat hunting on Western Lowland Gorillas," *EcoHealth*, vol. 4, no. 2, pp. 151–155, 2007.
- [8] T. W. Ng, G. Turinici, and A. Danchin, "A double epidemic model for the SARS propagation," *BMC Infect. Dis.*, vol. 3, no. 1, p. 19, 2003.
- [9] M. Small, P. Shi, and C. K. Tse, "Plausible models for propagation of the SARS virus," *IEICE Trans. Fund. Elect. Commu. Comput. Sci.*, vol. 87, no. 9, pp. 2379–2386, 2004.
- [10] O. Zakary, M. Rachik, and I. Elmouki, "On the impact of awareness programs in HIV/AIDS prevention: An SIR model with optimal control," *Int. J. Comput. Appl.*, vol. 133, no. 9, pp. 1–6, 2016.
- [11] S. Hochreiter and J. Schmidhuber, "Long short-term memory," *Neural Comput.*, vol. 9, no. 8, pp. 1735–1780, 1997.
- [12] T. Mikolov, M. Karafiát, L. Burget, J. Černocký, and S. Khudanpur, "Recurrent neural network based language model," in *Proc. Interspeech*, 2010, pp. 1045–1048.
- [13] K. Greff, R. K. Srivastava, J. Koutník, B. R. Steunebrink, and J. Schmidhuber, "LSTM: A search space Odyssey," *IEEE Trans. Neural Netw. Learn. Syst.*, vol. 28, no. 10, pp. 2222–2232, Oct. 2017.
- [14] F. A. Gers, J. Schmidhuber, and F. Cummins, "Learning to forget: Continual prediction with LSTM," *Neural Comput.*, vol. 12, no. 10, pp. 2451–2471, 2000.
- [15] K. Cho, B. van Merriënboer, D. Bahdanau, and Y. Bengio, "On the properties of neural machine translation: Encoder-decoder approaches," 2014. [Online]. Available: arXiv:1409.1259.
- [16] K. Cho *et al.*, "Learning phrase representations using RNN encoder-decoder for statistical machine translation," 2014. [Online]. Available: arxiv:1406.1078.
- [17] J. Du, C.-M. Vong, and C. L. P. Chen, "Novel efficient RNN and LSTM-like architectures: Recurrent and gated broad learning systems and their applications for text classification," *IEEE Trans. Cybern.*, early access, Feb. 20, 2020, doi: [10.1109/TCYB.2020.2969705](https://doi.org/10.1109/TCYB.2020.2969705).
- [18] J. Chung, K. Kastner, L. Dinh, K. Goel, A. C. Courville, and Y. Bengio, "A recurrent latent variable model for sequential data," in *Proc. Adv. Neural Inf. Process. Syst.*, 2015, pp. 2980–2988.
- [19] A. Graves, A.-R. Mohamed, and G. Hinton, "Speech recognition with deep recurrent neural networks," in *Proc. Int. Conf. Acoust. Speech Signal Process. (ICASSP)*, 2013, pp. 6645–6649.
- [20] T. Young, D. Hazarika, S. Poria, and E. Cambria, "Recent trends in deep learning based natural language processing," *IEEE Comput. Intell. Mag.*, vol. 13, no. 3, pp. 55–75, Aug. 2018.
- [21] A. van den Oord, N. Kalchbrenner, and K. Kavukcuoglu, "Pixel recurrent neural networks," 2016. [Online]. Available: arXiv:1601.06759.
- [22] A. Karpathy and L. Fei-Fei, "Deep visual-semantic alignments for generating image descriptions," in *Proc. Conf. Comput. Vis. Pattern Recognit. (CVPR)*, 2015, pp. 3128–3137.
- [23] Y. Bin, Y. Yang, F. Shen, N. Xie, H. T. Shen, and X. Li, "Describing video with attention-based bidirectional LSTM," *IEEE Trans. Cybern.*, vol. 49, no. 7, pp. 2631–2641, Jul. 2019.
- [24] X. Chen, J. Yu, and Z. Wu, "Temporally identity-aware SSD with attentional LSTM," *IEEE Trans. Cybern.*, early access, Feb. 11, 2019, doi: [10.1109/TCYB.2019.2894261](https://doi.org/10.1109/TCYB.2019.2894261).
- [25] G. Chowell, C. Castillo-Chavez, P. W. Fenimore, C. M. Kribs-Zaleta, L. Arriola, and J. M. Hyman, "Model parameters and outbreak control for SARS," *Emerg. Infect. Dis.*, vol. 10, no. 7, pp. 1258–1263, 2004.
- [26] C. Dye and N. Gay, "Modeling the SARS epidemic," *Science*, vol. 300, no. 5627, pp. 1884–1885, 2003.
- [27] N. Yoshida and T. Hara, "Global stability of a delayed SIR epidemic model with density dependent birth and death rates," *J. Comput. Appl. Math.*, vol. 201, no. 2, pp. 339–347, 2007.
- [28] N. Imai *et al.*, *Report 3: Transmissibility of 2019-nCoV*, WHO Collaborating Centre Infect. Dis. Model., MRC Centre Global Infect. Dis. Anal., J-IDEA, Imperial Coll. London, London, U.K., 2020. [Online]. Available: <https://doi.org/10.25561/77148>
- [29] S. F. Dowell, "Seasonal variation in host susceptibility and cycles of certain infectious diseases," *Emerg. Infect. Dis.*, vol. 7, no. 3, pp. 369–374, 2001.
- [30] (2020). *National Health Committee of the People's Republic of China*. Accessed: Feb. 3, 2020. [Online]. Available: <http://www.nhc.gov.cn>
- [31] J. Zhang, J. Lou, Z. Ma, and J. Wu, "A compartmental model for the analysis of SARS transmission patterns and outbreak control measures in China," *J. Comput. Appl. Math.*, vol. 162, no. 2, pp. 909–924, 2005.
- [32] B. Chen *et al.*, "Data visualization analysis and simulation prediction for COVID-19," 2020. [Online]. Available: arXiv:2002.07096.
- [33] J. A. Backer, D. Klinkenberg, and J. Wallinga, "Incubation period of 2019 novel Coronavirus (2019-nCoV) infections among travellers from Wuhan, China, 20–28 January 2020," *Euro Surveill.*, vol. 25, no. 5, 2020, Art. no. 2000062.

- [34] Y. Cui *et al.*, "Pre-training with whole word masking for chinese bert," 2019. [Online]. Available: [arxiv:1906.08101](https://arxiv.org/abs/1906.08101).
- [35] D. P. Kingma and J. Ba, "Adam: A method for stochastic optimization," 2014. [Online]. Available: [preprint arXiv:1412.6980](https://arxiv.org/abs/1412.6980).
- [36] I. Lin. (2020). *Real-Time Data API for COVID-19 Epidemic*. Accessed: Feb. 3, 2020. [Online]. Available: <https://lab.isaacclin.cn/nCoV/zh>
- [37] F. Zhang and X.-Q. Zhao, "A periodic epidemic model in a patchy environment," *J. Math. Anal. Appl.*, vol. 325, no. 1, pp. 496–516, 2007.
- [38] S.-L. Yuang, L. T. Han, and Z. E. Ma, "A kind of epidemic model having infectious force in both latent period and infected period," *J. Biomath.*, vol. 16, no. 4, pp. 392–398, 2001.
- [39] T. Zhang and D. Fang, "A kind of epidemic model with infectious force in both latent period and infected period and nonlinear infection rate," *J. Biomath.*, vol. 21, no. 3, pp. 345–350, 2006.



Nanning Zheng (Fellow, IEEE) received the graduation degree from the Department of Electrical Engineering, Xi'an Jiaotong University, Xi'an, China, in 1975, and the M.S. degree in information and control engineering from Xi'an Jiaotong University in 1981, and the Ph.D. degree in electrical engineering from Keio University, Yokohama, Japan, in 1985.

He joined Xi'an Jiaotong University in 1975, where he is currently a Professor and the Director of the Institute of Artificial Intelligence and Robotics.

His research interests include computer vision, pattern recognition, and machine learning.

Prof. Zheng is the Chinese Representative on the Governing Board of the International Association for Pattern Recognition. He also serves as the President of the Chinese Association of Automation. He became a member of the Chinese Academy of Engineering in 1999.



Shaoyi Du (Member, IEEE) received the double B.S. degrees in computational mathematics and in computer science, the M.S. degree in applied mathematics, and the Ph.D. degree in pattern recognition and intelligence systems from Xi'an Jiaotong University, China, in 2002, 2005, and 2009, respectively.

He was a Postdoctoral Fellow with Xi'an Jiaotong University from 2009 to 2011, and visited the University of North Carolina at Chapel Hill, Chapel Hill, NC, USA, from 2013 to 2014. He is currently

a Professor with Xi'an Jiaotong University. His research interests include machine learning, medical image analysis, computer vision, and pattern recognition.



Jianji Wang (Member, IEEE) received the B.S. degree in applied mathematics, the M.E. degree in computer science and technology, and the Ph.D. degree in control science and engineering from Xi'an Jiaotong University, Xi'an, China, in 2003, 2007, and 2013, respectively.

He was a Visiting Scholar with the Computational NeuroEngineering Laboratory, University of Florida, Gainesville, FL, USA, from 2016 to 2017. He is currently an Associate Professor with the Institute of Artificial Intelligence and Robotics, Xi'an Jiaotong

University. His research interests include image processing, machine learning, and correlation analysis.



He Zhang received the B.S. degree from the School of Electronic and Information Engineering, Xi'an Jiaotong University, Xi'an, China, in 2019, where he is currently pursuing the Ph.D. degree.

His research interests include machine learning and computational biology.



Wenting Cui received the B.S. degree in computer science and technology from Tiangong University, Tianjin, China, in 2015, and the M.S. degree from the School of Software Engineering, Xi'an Jiaotong University, Xi'an, China, in 2019, where she is currently pursuing the Ph.D. degree.

Her research interests include machine learning, medical image analysis, and pattern recognition.



Zijian Kang received the B.S. degree from the School of Electronic and Information Engineering, Xi'an Jiaotong University, Xi'an, China, in 2019, where he is currently pursuing the M.S. degree.

His research interests include machine learning and computer vision.



Tao Yang received the B.S. degree from the School of Electronic and Information Engineering, Xi'an Jiaotong University, Xi'an, China, in 2019, where he is currently pursuing the Ph.D. degree.

His research interests include generative models and representation learning.



Bin Lou received the B.S. degree in software engineering from Chang'an University, Xi'an, China, in 2018. He is currently pursuing the M.S. degree with Xi'an Jiaotong University, Xi'an.

His research interests include machine learning and natural language processing.



Yuting Chi received the B.S. degree in software engineering from Jiangxi Normal University, Nanchang, China, in 2017. She is currently pursuing the M.S. degree with Xi'an Jiaotong University, Xi'an, China.

Her research interests include machine learning and medical image analysis.



Hong Long received the B.S. degree in printing engineering from the Xi'an University of Technology, Xi'an, China, in 2017. She is currently pursuing the M.S. degree with Xi'an Jiaotong University, Xi'an.

Her research interests include machine learning and medical image analysis.



Mei Ma received the B.S. degree from the School of Electronic and Information Engineering, Xi'an Jiaotong University, Xi'an, China, in 2018, where she is currently pursuing the M.S. degree.

Her research interests include deep learning and natural language processing.



Dong Zhang received the B.S. degree in electronic information science and technology, and the M.S. degree in pattern recognition and intelligent systems from the Lanzhou University of Technology, Lanzhou, China, in 2014 and 2019, respectively.

He is currently an intern with Xi'an Jiaotong University, Xi'an, China. His research interests include machine learning and medical image analysis.



Qi Yuan received the B.S. degree from the School of Electronic and Information Engineering, Xi'an Jiaotong University, Xi'an, China, in 2019, where he is currently pursuing the M.S. degree.

His research interests include deep learning and computer vision.



Feng Ye received the B.M. degree from Xi'an Medical University, Xi'an, China, in 1997, and the M.S. and Ph.D. degrees from Xi'an Jiaotong University, Xi'an, in 2002 and 2005, respectively.

He was a Visiting Scholar with Johns Hopkins University, Baltimore, MD, USA, and the University of Oklahoma, Norman, OK, USA, from 2016 to 2017. He is currently a Chief Physician with the First Affiliated Hospital of Xi'an Jiaotong University, Xi'an. His research interests include the mother-to-child transmission of HBV, fatty liver, and severe hepatitis.



Shupeizhang received the B.E. degree in software engineering from Xidian University, Xi'an, China, in 2019. He is currently pursuing the M.S. degree with Xi'an Jiaotong University, Xi'an.

His research interests include image in painting and computer vision.



Jingmin Xin (Senior Member, IEEE) received the B.E. degree in information and control engineering from Xi'an Jiaotong University, Xi'an, China, in 1988, and the M.S. and Ph.D. degrees in electrical engineering from Keio University, Yokohama, Japan, in 1993 and 1996, respectively.

From 1988 to 1990, he was with the Tenth Institute of Ministry of Posts and Telecommunications, Xi'an. He was an Invited Research Fellow of the Telecommunications Advancement Organization of Japan with the Communications Research Laboratory, Tokyo, Japan, from 1996 to 1997, and a Postdoctoral Fellow with the Japan Science and Technology Corporation, Kawaguchi, Japan, from 1997 to 1999. He was also a Guest (Senior) Researcher with YRP Mobile Telecommunications Key Technology Research Laboratories Company Ltd., Yokosuka, Japan, from 1999 to 2001. From 2002 to 2007, he was with Fujitsu Laboratories Ltd., Yokosuka. Since 2007, he has been a Professor with Xi'an Jiaotong University. His research interests include the areas of adaptive filtering, statistical and array signal processing, system identification, and pattern recognition.